

Latin American Journal of Sedimentology and Basin Analysis

ISSN 1851-4979

Published by the Asociación Argentina de Sedimentología

ACCEPTED MANUSCRIPT

Unveiling a landscape: mapping aeolian dunes in the Argentine Pampa plain using local entropy analysis of DEMs

Rafael Grimson , Daniela Negro Sirch , Alfonsina Tripaldi 

Received date: 19-11-2025

Accepted date: 18-05-2026

Available online: 03-06-2026

Handling Editor: Valentina Flores Aqueveque

Please cite this article as

Grimson, R., Negro Sirch, D., and Tripaldi, A. Unveiling a landscape: mapping aeolian dunes in the Argentine Pampa plain using local entropy analysis of DEMs (in press). *Latin American Journal of Sedimentology and Basin Analysis*.

This is a preliminary version of the manuscript accepted for publication in the Latin American Journal of Sedimentology and Basin Analysis. This version will be revised before final publication. Please note that some errors may be found during the final revision process. The same disclaimers as for printed and final versions apply for this early online version.

Asociación Argentina de Sedimentología

This work is licensed under Creative Commons Attribution-NonCommercial 2.5 Argentina License

Unveiling a landscape: mapping aeolian dunes in the Argentine Pampa plain using local entropy analysis of DEMs

Grimson, R.^{1*}, Negro Sirch, D.^{2,3,4}, Tripaldi, A.^{3,4}

1 – Instituto de Investigación e Ingeniería Ambiental (IIA), Escuela de Hábitat y Sostenibilidad, Campus Migueletes, Universidad Nacional de San Martín (UNSAM). 25 de Mayo y Francia n° 1650, San Martín, Argentina.

2 – Centro de Estudios Integrales de la Dinámica Exógena (CEIDE), Universidad Nacional de La Plata (UNLP). Calle 64 n° 3 (1900), La Plata, Argentina.

3 – Universidad de Buenos Aires (UBA), Facultad de Ciencias Exactas y Naturales, Departamento de Ciencias Geológicas. Intendente Güiraldes n° 2160 (C1428EHA), Buenos Aires, Argentina.

4 – Consejo Nacional de Investigaciones Científicas y Tecnológicas (CONICET), Universidad de Buenos Aires (UBA), Instituto de Geociencias Básicas, Aplicadas y Ambientales de Buenos Aires (IGEBA). Intendente Güiraldes n° 2160 (C1428EHA), Buenos Aires, Argentina.

*Corresponding author: rgrimson@unsam.edu.ar

ABSTRACT

The Pampa plain of Argentina, southern South America, constitutes a vast low-relief landscape whose Neogene-Quaternary history was dominated by aeolian deposition and morphogenesis. Although dunes exist in the region—mostly inactive under current climatic conditions—their full spatial extent and morphology have remained partially obscured by vegetation (grassland) and agricultural activity, rendering them difficult to detect with conventional digital elevation model (DEM) visualization techniques. To address this challenge, we developed DemEntropy, a novel method that applies a local entropy filter to a DEM to quantify topographic disorder and highlight organized geomorphic patterns. This open-source software package is freely

distributed and provides a reproducible method for enhancing subtle topographic features based on their textural properties. Application of DemEntropy to TanDEM-X data for the Pampa plain yielded two significant results. First, it successfully enhanced the boundaries and aeolian morphologies of the known Central Pampean Dunefield unit (CPD), of the Pampean Sand Sea, demonstrating the robustness of the method. Second, and more notably, it revealed extensive, previously undocumented aeolian features northeast of the Tandilia range, in the loess domain (Loess and loess-like mantles and blowouts unit, LMB), where such features are not discernible in standard hillshade models. These findings demonstrate the efficacy of local entropy analysis for geomorphological mapping and reveal a more complex and extensive history of aeolian activity in the region than previously recognized. By providing this tool as a freely available software package, we aim to enable the wider community to apply this powerful technique to the study of subtle aeolian and fluvial landscapes in other vegetated and low-relief settings globally.

Keywords: Remote sensing, Local Entropy, Parabolic dunes, Quaternary, TanDEM-X

INTRODUCTION

The Pampa plain of Argentina, southern South America, is one of the world's most extensive loess- and loess-like-covered regions and, together with associated stabilized dunefields to the west, represents a critical record for understanding the Neogene-Quaternary evolution of southern South America. The geomorphological evolution of this plain has been profoundly influenced by aeolian processes, including both the construction of sand dunefields and the deposition of silty loess mantles, known as the Pampean Sand Sea and Peripheral Loess Belt, respectively (Iriondo and Kröhling, 1995). This aeolian morphogenesis was locally associated with fluvial processes along the few rivers crossing this plain, and lacustrine sedimentation in wetlands and shallow lakes (Zárate, 2009). The Pampean aeolian system underwent

successive periods of reworking, erosion, stabilization, and greening, the last of which occurred during the latest Holocene (Tripaldi *et al.*, 2025 and references therein). In addition, significant anthropogenic land modification has occurred over the past 120 years, mainly due to agriculture (Viglizzo and Frank 2006).

While some previous studies characterized the dune patterns in different areas of the Pampean aeolian cover (*e.g.*, Malagnino, 1989; Martínez *et al.*, 2001; Zárate and Mehl, 2010; Contreras *et al.*, 2018; Messineo *et al.*, 2019; Tripaldi *et al.*, 2025), the full spatial distribution and morphological types of these aeolian landscapes remain to be mapped in detail. In particular, many aeolian features are of low amplitude (<3 m), heavily vegetated, or partially modified by agriculture, rendering them subtle and difficult to detect. This mapping challenge is not unique to the Argentine Pampa but is a common problem in geomorphology where dunes are preserved in vegetated, low-relief settings.

Traditional techniques for visualizing digital elevation models (DEMs), such as hillshading and slope maps, are often inadequate for this task. Hillshading is highly sensitive to illumination azimuth and can fail to reveal features aligned parallel to the light source, while slope maps may fail to distinguish low-amplitude, large-wavelength features from flat surrounding terrain. Consequently, there is a persistent need for robust, quantitative analytical techniques that can enhance the visibility of subtle geomorphic patterns based on their fundamental properties rather than their absolute relief. Recent advances in quantitative geomorphometry include the application of texture statistics to DEMs for dune classification, as demonstrated by Almutlaq and Mulligan (2023) in the Rub' al Khali, underscoring the potential of texture-based approaches for aeolian landscape analysis.

Moreover, as evidenced by recent reviews of remote sensing advances in aeolian geomorphology (Zheng *et al.*, 2022), there is growing recognition that detecting wind-accumulation landforms in vegetated settings requires moving beyond conventional visualization methods. One promising approach lies in

the application of concepts from information theory, specifically the measure of entropy as defined by Shannon (1948). In a geomorphological context, entropy can be used to quantify the spatial disorder or complexity of a topographic surface. We hypothesize that organized geomorphic patterns, such as those produced by aeolian dune activity, present a distinct entropy signature compared to flat terrain. A field of dunes exhibits a repetitive, structured texture that should correspond to a specific, predictable range of local entropy values, acting as a diagnostic fingerprint even after the features have been subdued and vegetated.

To test this hypothesis and provide the community with a practical tool, we developed DemEntropy, an open-source Python package designed specifically for the computation and application of local entropy to DEMs. This paper has two primary objectives. First, we present the DemEntropy software package, detailing its algorithmic basis and its implementation as an accessible and reproducible tool. Second, we demonstrate its application to the TanDEM-X DEM of the Pampa plain. Our analysis not only enhances the mapping of known aeolian features but, more significantly, reveals the presence of previously undocumented extensive aeolian landforms northeast of the Tandilia range. These results provide new evidence for reevaluating the region's aeolian history and showcase the value of local entropy analysis as a powerful new technique in the geomorphological toolkit.

GEOLOGICAL SETTING

The Pampa plain of Argentina is a vast sedimentary basin characterized by its low-relief topography, except for the low hills of the Tandilia and Ventania ranges, and a Neogene-Quaternary history dominated by aeolian processes, accompanied by local fluvial activity and wetland-lacustrine sedimentation (Zárate, 2009 and references therein). The region is predominantly blanketed by a stabilized aeolian cover, with loess and loess-like sediments to the east and sand and silty sand in central and western Pampa (Iriondo and Kröhling, 1995; Zárate, 2003), shaped into varied landforms (Zárate and Tripaldi, 2012).

This geodiversity led to the proposal of a classification of the aeolian system of central Argentina, which includes a series of regional units characterized by different dune morphologies, erosive landforms, variable sediment types, and diverse morphostructural settings (Zárate and Tripaldi, 2012; Fig. 1). The dunefields and loess-loessial mantles of central Argentina attest to widespread past aeolian activity under drier climatic conditions (Tripaldi and Zárate, 2016) and episodes of erosion-reworking, stabilization, and pedogenesis along the Neogene-Quaternary (Zárate, 2005). At present, the aeolian landscape is mostly stabilized by extensive agriculture fields, with some remains of anthropogenically modified Pampean grassland (Oyarzabal *et al.*, 2018).

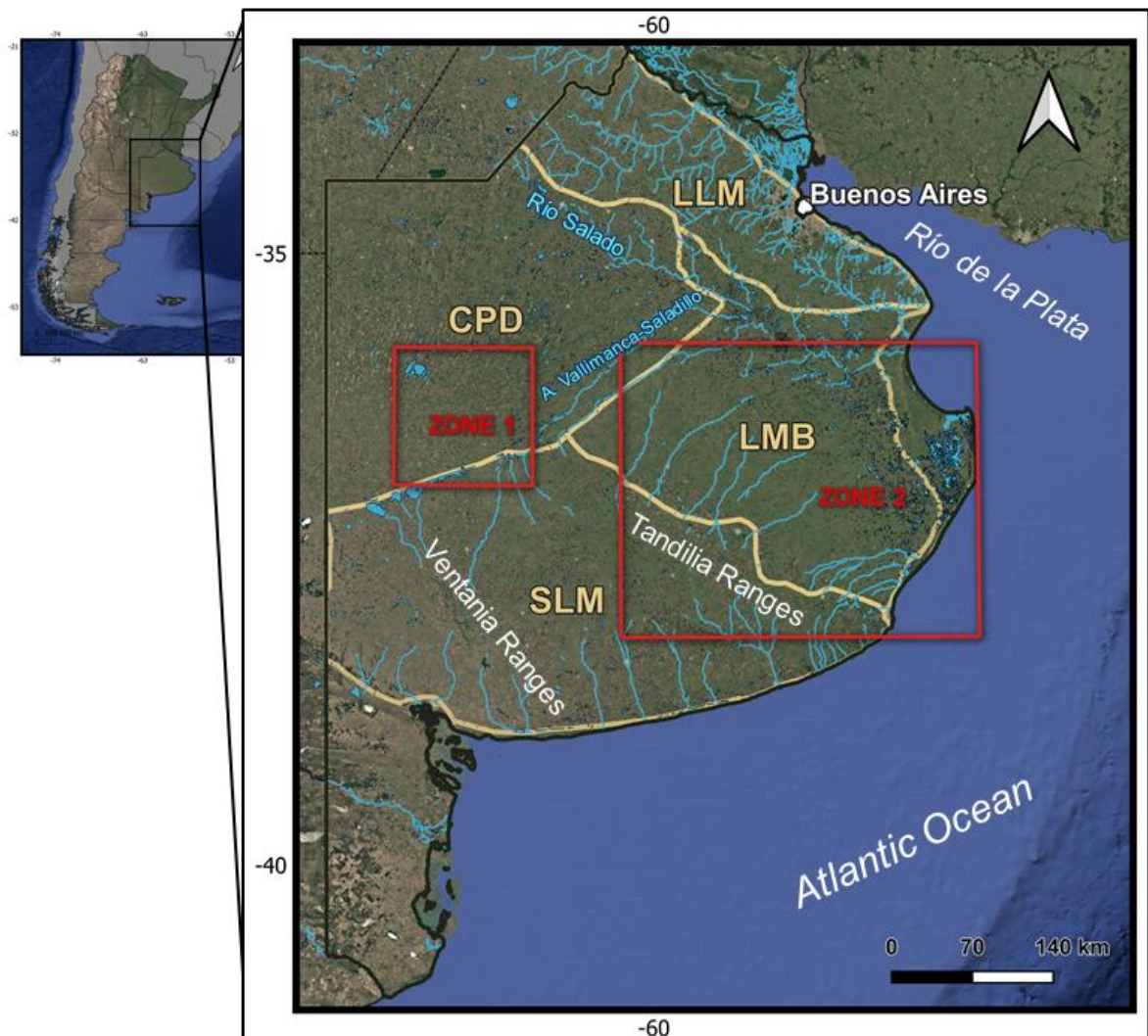


Figure 1. Location map of the study areas within the Pampa Plain (Buenos Aires Province, Argentina). The red rectangles mark the Zone 1 (evaluation) and Zone 2 (discovery) located in the Aeolian System of central Argentina. The background is a Google Satellite image showing

the land cover context, the main drainage systems, and the boundaries (yellow lines) of the aeolian units in the Buenos Aires Province (after Zárata and Tripaldi, 2012). Those aeolian units are Loess and loess-like mantles (LLM), Loess and loess-like mantles and blowouts (LMB), Sandy loess and loessial sand mantles (SLM), and Central Pampean dunefields (CPD; contours after Tripaldi *et al.*, 2025).

The recognition and mapping of the Pampean aeolian landscapes have been the subject of numerous studies since the pioneering work of Frenguelli (1955). In the Pampa plain of the Buenos Aires Province, there are two aeolian units relevant to this study. On the one hand, in the Central Pampean Dunefield unit (CPD), located in the area informally known as Pampa Arenosa (sandy Pampa), several authors mapped longitudinal and parabolic dunes (Malagnino, 1989; Contreras *et al.*, 2018; Messineo *et al.*, 2019; Tripaldi *et al.*, 2025). On the other hand, in the Loess and loess-like mantles and blowouts unit (LMB), in the area informally referred to as Pampa Deprimida (low Pampa), the dominant aeolian landforms are irregular and low-topography loess and loessial mantles and blowouts, the latter commonly occupied by shallow lakes (Tricart, 1973) associated with lunette dunes (Dangavs, 1979). Other dune types have only rarely been reported; in a few sectors of the northern piedmont of the Tandilia range some linear and parabolic dunes were recognized (Martínez *et al.*, 2001; Zárata and Mehl, 2010).

Associated with the aeolian landforms, wetlands and shallow lakes are widespread in the Pampa plain. These water bodies are significant for multiple reasons: they contribute to ecohydrological, hydrogeological, and limnological studies; serve as repositories of Quaternary records; act as sensors of global change; and function as water reservoirs (Piovano *et al.*, 2025). These shallow lakes are mostly of aeolian origin, linked to deflation (blowouts, pans, and lunettes) and to dune accumulation and migration (parabolic dunes, blowout dunes) (Tripaldi *et al.*, 2025 and references therein). In this sense, the development of new remote sensing techniques for improving the mapping of aeolian landforms becomes relevant not only for aeolian studies but also for recognizing potential areas subject to the development of wetlands and shallow lakes. Furthermore, by highlighting organized geomorphic and hydrological patterns within seemingly uniform

plains, the DemEntropy tool provides a valuable methodology for delineating landscapes with homogeneous characteristics, thereby offering a reproducible technique to support systematic landform inventorying initiatives such as the National Wetlands Inventory of Argentina (Benzaquén *et al.*, 2020).

METHODOLOGY

Algorithm Design and Implementation

The DemEntropy algorithm is grounded in Shannon's information entropy (Shannon, 1948), which serves as a measure of disorder or complexity within a dataset. When applied to digital elevation models (DEMs), terrain entropy quantifies the spatial heterogeneity of topographic surfaces. Highly heterogeneous terrain, characterized by strong topographic variability, yields high entropy values, while homogeneous flat surfaces exhibit minimal entropy. Notably, organized geomorphic patterns —such as the repetitive texture of dunefields— occupy an intermediate state, presenting a structured complexity that generates a distinct entropy signature.

This theoretical framework posits that aeolian features, at present stabilized by vegetation, even when topographically subdued, retain a textural organization that can be quantified through local entropy analysis. Unlike traditional DEM visualization techniques that rely on absolute elevation or first-derivative measures like slope, entropy analysis focuses exclusively on the spatial distribution of values, making it particularly powerful for detecting subtle organized patterns in low-relief landscapes.

To provide a standardized and reproducible implementation of this approach, we developed DemEntropy as an open-source Python package. The software is released under the MIT license, is platform-independent, and can be installed directly from the Python Package Index (PyPI) using the command `pip install dementropy`. The source code is freely available through PyPI, ensuring full accessibility for academic use.

The core algorithm processes a DEM through two stages. First, in a discretization step, continuous elevation values are converted into a finite number of integer bins. This conversion is controlled by two parameters: δ , which defines the height interval of each bin, and $nbits$, which determines the number of bins (2^{nbits}). The resulting integer grid represents the topographic signal as a series of discrete symbolic values. Second, in the local entropy calculation step, Shannon entropy is computed within a moving window of radius r (in pixels) defined by a circular structuring element (a disk). For each pixel, the entropy H is obtained from the probability distribution of the discrete values within its neighborhood:

$$\text{eq. (1) } H = -\sum p(i)\log(p(i))$$

where $p(i)$ is the probability of the i -th discrete value occurring in the window. This computation is performed efficiently using the entropy function from the *skimage* module (Van der Walt *et al.*, 2014). The algorithm also incorporates an optional shift-averaging procedure, which runs the calculation multiple times with slight vertical offsets and then averages the results, thereby minimizing quantization artifacts and producing a more robust output.

The software implementation relies on the Python scientific ecosystem, using *rasterio* for geospatial data handling and *scikit-image* for entropy computation. A command-line interface (CLI) accepts the path to the input DEM and key parameters: the radius ($-r$), the discretization interval ($-\delta$), and the number of bits for value range ($-nbits$). An optional $-\text{shift}$ flag invokes the averaging procedure. For rapid visualization, the tool can also generate a stretched PNG preview of the results. The output is a georeferenced entropy raster in GeoTIFF format that preserves the original spatial reference system, allowing direct integration into any Geographic Information System.

Selection of study areas

To demonstrate the efficacy of the DemEntropy tool in mapping dune morphology and geomorphological features, this study focuses on two distinct areas within the Pampa Plain (Zone 1 and Zone 2 in Fig. 1).

Zone 1 (Evaluation Site), in a sector of the CPD aeolian unit, was selected as a reference site because it contains well-documented, previously mapped aeolian dunes (Malagnino, 1989; Contreras *et al.*, 2018; Messineo *et al.*, 2019; Tripaldi *et al.*, 2025). Applying DemEntropy here allows for a direct comparison between the tool's output and existing geomorphological knowledge, providing a robust evaluation of its performance in a landscape where features are known to exist.

Zone 2 (Discovery Site), in the northeastern Tandilia range and comprising a sector of the LMB aeolian unit, was chosen precisely because it appears as a seemingly flat, featureless plain in conventional DEM visualizations (hillshade, slope maps). The lack of previously reported significant aeolian features, except for two local examples (Martínez *et al.*, 2001; Zárata and Mehl, 2010), makes Zone 2 an ideal testing ground to assess the method's power to reveal subtle, potentially unknown, geomorphic patterns.

Data Acquisition and Preprocessing

The primary data source for this analysis was the TanDEM-X 90m DEM product (Wessel, 2018) at a spatial resolution of 3 arc-second (approximately 90 meters). This dataset was selected for its near-global coverage, consistency, and suitability for regional-scale geomorphological mapping. Although higher-resolution DEMs (*e.g.*, 30 m) are also available, preliminary comparisons did not reveal significant improvements in capturing the aeolian patterns of interest, confirming the 90 m product as adequate for the target landform scale. For finer-scale features, however, higher-resolution topographic data may be more appropriate. The TanDEM-X imagery used in this study is freely accessible and can be downloaded directly from the German Aerospace Center (DLR) portal. The specific TanDEM-X tiles covering the area of interest were downloaded and mosaicked as needed. The use of a

widely available global DEM underscores the reproducibility of this method, as any researcher can access the identical input data.

Application of the DemEntropy Algorithm

The DemEntropy package was applied to the prepared TanDEM-X regional DEM to generate local entropy maps for both study areas. The operational parameters, δ and r , were selected through a preliminary sensitivity analysis to optimize the detection of large-scale aeolian features characteristic of the Pampa plain, based on a grid search. The outcomes are presented in the Results section. The best parameter combination was identified through visual comparison of the resulting entropy maps, balancing feature delineation and noise suppression.

The calculation utilized an 8-bit symbolic representation and incorporated the shift-averaging procedure to minimize potential quantization artifacts introduced by the discretization step. This approach produced robust entropy maps with smooth transitions between different textural domains. Execution of the algorithm on the mosaicked TanDEM-X data for both Zone 1 (evaluation) and Zone 2 (discovery) generated georeferenced entropy rasters in GeoTIFF format as primary outputs, where each pixel value represents the computed local entropy of the original topography. These rasters were incorporated as GIS layers and served as the fundamental data source for all subsequent geomorphological interpretation and analysis described in the following sections.

Evaluation and Interpretative Framework

The evaluation of the results was conducted through a multi-step interpretative process. The primary output, a georeferenced entropy map, was first visually compared against widely used terrain visualization techniques (Morley *et al.*, 2025): Standard hillshade (HS), sky-view factor (SVF; Zakšek *et al.*, 2011), and simple local relief models (SLR; Hesse, 2010) generated from the same TanDEM-X DEM. This direct comparison served to highlight the visibility of textural patterns in the entropy map. The SVF and SLR models

were computed using the relief visualization Toolbox QGIS plugin (Kokalj and Somrak, 2019).

These patterns were then examined and interpreted in terms of aeolian geomorphology, following classical dune classifications (Melton, 1940; McKee, 1979) as well as a recently revisited proposal (Courrech du Pont *et al.*, 2024). The analysis was focused on identifying organized, repetitive patterns within the entropy landscape —such as alignments, crests, and slipface orientations— that are diagnostic of aeolian bedforms. This visual interpretation of the entropy-derived textures constitutes the core methodology for evaluating the features revealed by the DemEntropy tool, bridging quantitative analysis with qualitative geomorphological expertise. Published sedimentological data from in-situ surveys were also considered to support the interpretations.

RESULTS

Sensitivity analysis of parameters

The operational parameters, δ and r , were selected through a grid search with δ ranging from 0.1 m to 1.0 m in 0.1 m increments and r ranging from 1 to 5 pixels (Fig. 2b-f). Figure 2a shows an RGB satellite image of the representative sector, illustrating the cultivated fields and grassland that obscure the aeolian features; panels (b–f) present the corresponding entropy maps for different parameter combinations. Visual comparison of the resulting entropy maps showed that $\delta = 0.5$ m and $r = 2$ pixels (Fig. 2b) provided the best balance between feature delineation and noise suppression. Values of δ smaller than 0.5 m introduced excessive discretization noise (Fig. 2c), while larger values smoothed out subtle topographic variations (Fig. 2d). Regarding r , a radius of 1 pixel produced overly detailed, noisy patterns (Fig. 2e), whereas $r = 5$ pixels blurred the dune borders, losing ridge definition (Fig. 2f). The selected $r = 2$ pixels corresponds to 180 m at the native 90 m resolution, aligning with the typical wavelength of Pampean dunefield ridges. The value

of $\delta = 0.5$ m is smaller than the expected amplitude of the target dunes, ensuring that subtle vertical variations were meaningfully captured without excessive quantization.

For these fixed parameters, the DemEntropy algorithm was applied to two study cases in the Pampa plain: an evaluation site, Zone 1, with known dunes of the CPD aeolian unit, and a discovery site, Zone 2, covering a sector of the LMB aeolian unit that had not been previously characterized with dune bedforms (Fig. 1). The results for the two study areas are presented below.

DemEntropy algorithm for enhancement of known features

The entropy map of Zone 1, from a sector of the CPD unit, produced a noticeably enhanced representation of the known dunes (Tripaldi *et al.*, 2025 and references therein; Fig. 3). Whereas hillshade and sky-view factor models render these features as faint, amorphous tonal variations (Fig. 3a–b), the local entropy calculation sharpened their boundaries and elucidated their internal organization (Fig. 3c). The grayscale visualization clearly delineates extensive areas of low entropy (dark pixels) corresponding to flat plains, juxtaposed against well-defined linear and curvilinear ridges of higher entropy (light pixels). The simple local relief model also reveals the dune boundaries (Fig. 3d), albeit with a different textural emphasis: SLR highlights relative elevation differences, while entropy emphasizes the spatial organization of the pattern.

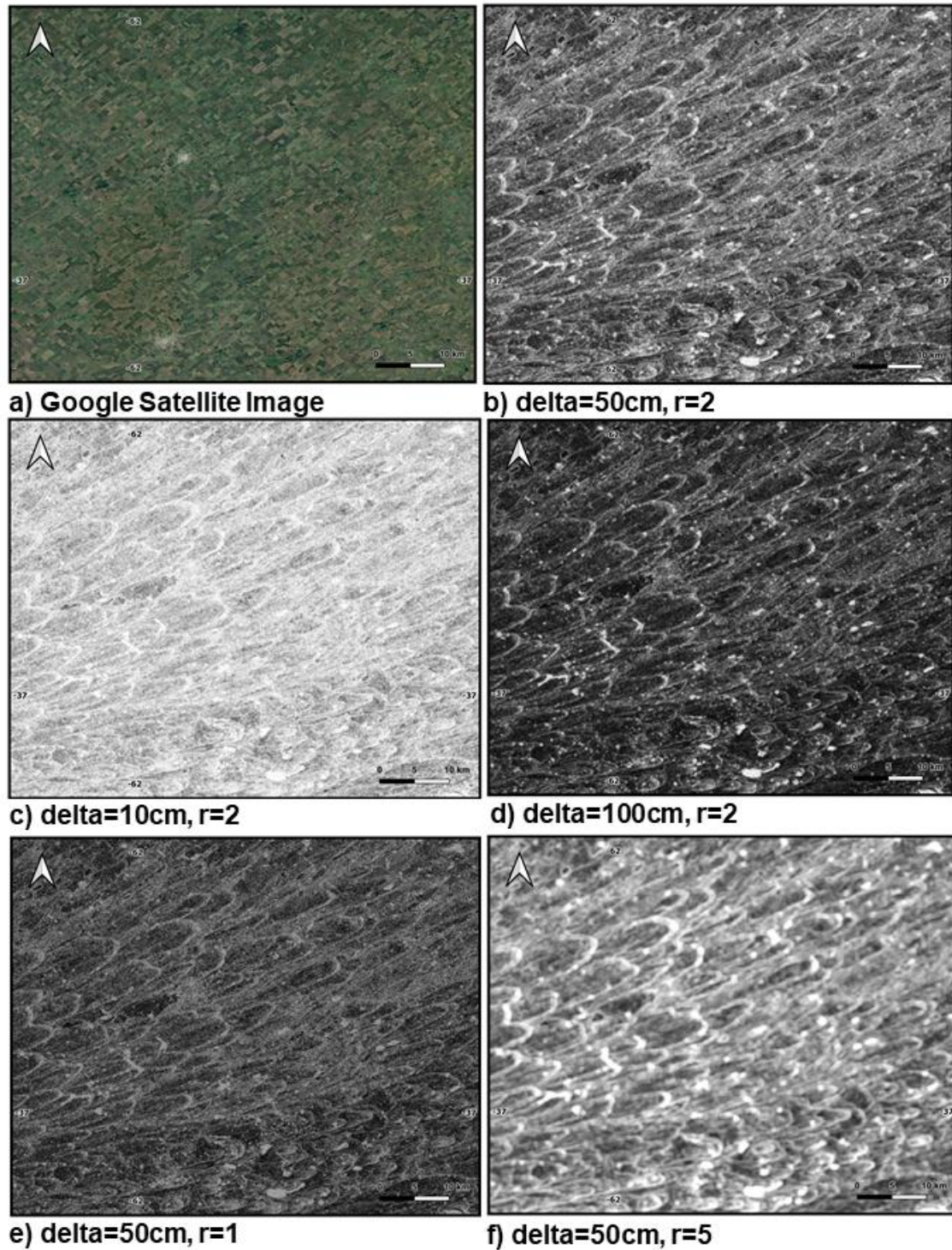


Figure 2. Sensitivity analysis of the DemEntropy parameters. **a)** RGB satellite image (Google Satellite) of the representative sector of Zone 1, showing cultivated fields and grassland where aeolian dunes are not discernible. (**b–f**) Entropy maps illustrating the effect of varying δ and r on the same sector. **b)** $\delta = 0.5 \text{ m}$, $r = 2$ (selected configuration). **c)** $\delta = 0.1 \text{ m}$, $r = 2$ (discretization noise dominates). **d)** $\delta = 1.0 \text{ m}$, $r = 2$ (excessive quantization, loss of subtle features). **e)** $\delta = 0.5 \text{ m}$, $r = 1$ (noisy, overly detailed). **f)** $\delta = 0.5 \text{ m}$, $r = 5$ (oversmoothed,

individual ridges merge). The selected parameters (b) best capture the organized dune texture, which remains undetectable in the satellite image.

The high-entropy map exhibits a linear pattern associated with curvilinear ribbons, which agrees with the geomorphological characteristics of parabolic dunes, where the linear ridges represent the dune arms and those arms are close in a hook denoting the dune nose (elongated simple parabolic dune sketch in Fig. 3f). Like in optical satellite images, no stream channels appear in the entropy map (Fig. 3c). The profuse presence of high entropy values (lighter pixels) in the form of arcs is considered a diagnostic feature for assuming the presence of parabolic dunes. Moreover, the entropy map allows the recognition of different subtypes within the analyzed area, that is, simple parabolic dunes (elongated type) and compound parabolic dunes, including the subtypes nested, en-echelon, digitate, and superimposed parabolic dunes (after Pye, 1993; Fig. 3c).

The map of Zone 1 also reveals a high density of parabolic dunes to the north of the Lagunas Encadenadas del Oeste (Fig. 3c), where the dune pattern presents numerous dune noses closely associated and/or nested within one another, rather than few noses followed by long arms. The entropy map exposes a coherent dune alignment, with the nose convex indicating sand transport towards the NE (Fig. 3c).

DemEntropy algorithm for discovery of novel features

The analysis of Zone 2, covering a large sector of the LMB aeolian unit, presented a far more significant outcome. There, the difference between the standard hillshade models and the entropy map is more pronounced (Fig. 4). In this sector, the standard hillshade model (Fig. 4a) depicts a seemingly homogeneous and largely featureless plain, offering little suggestion of underlying extensive geomorphic organization. The sky-view factor models neither show a relevant organization (Fig. 4b). The application of the DemEntropy tool, however, revealed a strikingly different landscape. The resulting map (Fig. 4c) uncovered a vast and previously undocumented assemblage of landforms characterized by a distinct textural signature. These

features manifest as a well-organized set of elongated, high-entropy ribbons that form expansive, overlapping fields. Their morphology includes both linear and gently curvilinear patterns, with a predominant east-west orientation. The clarity, spatial extent and geometric regularity of these features in the entropy map stand in stark contrast to their subtle expression in the traditional hillshade and sky-view factor models, underscoring the capability of the local entropy method to extract subtle geomorphic information from a low-relief topographic surface. Surprisingly, the local relief model (Fig. 4d) also highlights these undocumented structures.

The entropy map of Zone 2 encompasses the northeastern piedmont of the Tandilia ranges, characterized by a 0.3% slope towards the northeast and covered by loess and loess-like mantles. Similarly to the map of Zone 1, in the area north of the ranges, well-organized set of elongated, high-entropy ribbons resembles the morphology of parabolic dunes, where the linear ridges (arms) close into curvilinear ridges (noses). The linear features are continuous for tens of kilometers, with a homogeneous SW-NE orientation, and, significantly, they cross the directions of the small arroyos that drain the Tandilia ranges (Fig. 4c). Subsequently, a reasonable interpretation is that these landforms also respond to aeolian processes, in the form of parabolic dunes. This inference is supported by the presence of curved ridges, interpreted as the dune nose (Fig. 4c). These curved ridges are convex towards the NE, indicating a common northeasterly sediment transport like the one denoted by the parabolic dunes of Zone 1 (Fig. 3).

The parabolic dune pattern in the LMB unit is somewhat different and more variable in size than that in the Zone 1 area; it also exhibits greater morphological diversity. In the northern sector of Zone 2 (Fig. 4c) the dune arms extend for several kilometers; here the most common type is the digitate parabolic dunes (Fig. 4c). In comparison, in the southern sector the pattern of parabolic dunes is more subtle, and, although present, there are fewer curvilinear noses (Fig. 4c). However, these high-entropy ridges are also interpreted as a parabolic dune pattern. In the entropy map of Zone 2, the parabolic dune pattern terminates approximately 15 to 70 km westward of the

Atlantic coast, where the LMB aeolian unit (Tripaldi *et al.*, 2025) transitions to marshes and marine coastal plain deposits.

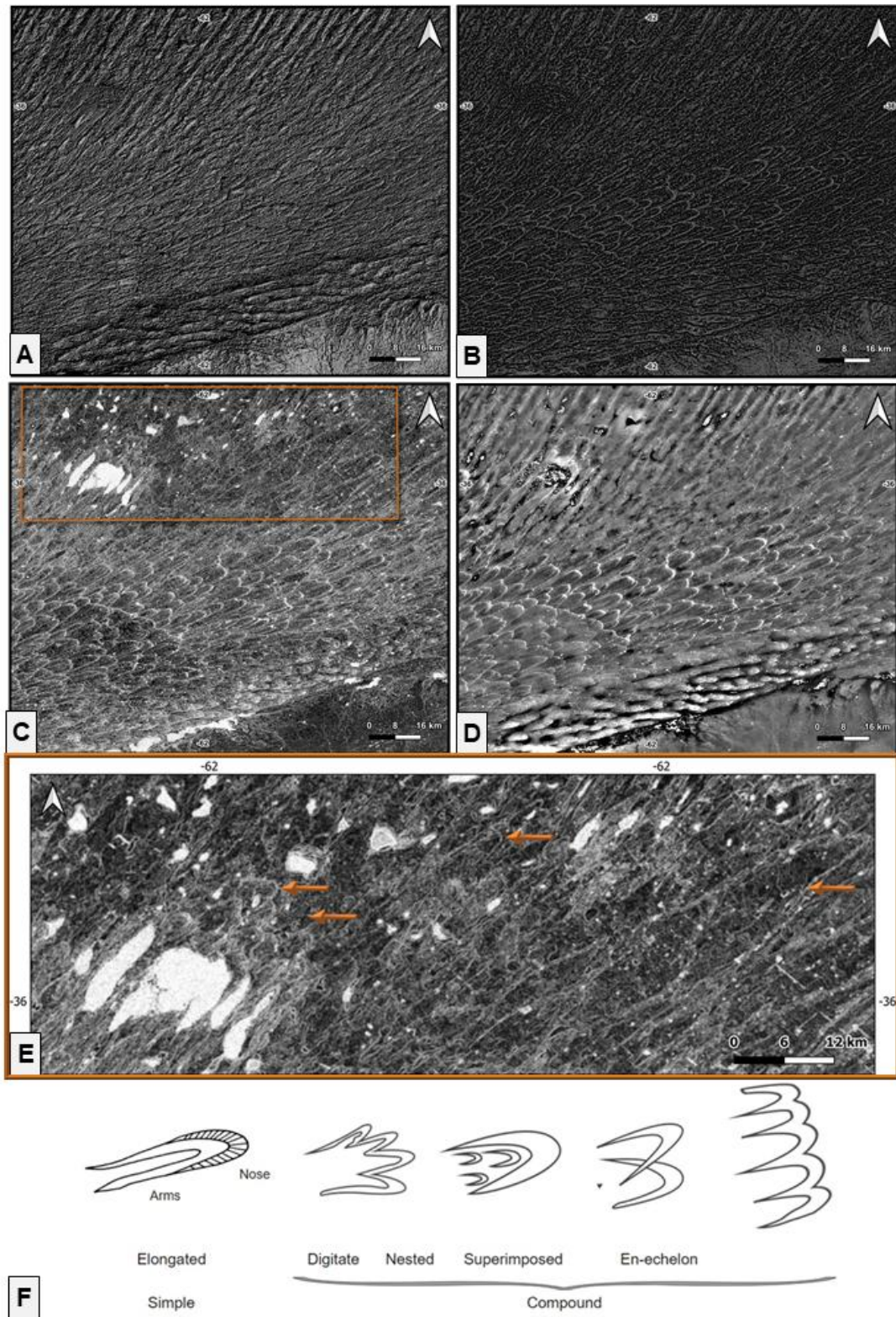


Figure 3. Application of the local entropy method to the CPD aeolian unit (Zone 1 in Fig. 1), where parabolic dunes were previously documented (Tripaldi *et al.*, 2025, and references therein). **a)** Standard hillshade model (azimuth 315°). Aeolian features are faint and poorly defined. **b)** Sky-view factor (SVF) map; features remain difficult to perceive. **c)** Local entropy map ($r = 2$ pixels, $\delta = 0.5$ m). Dune ridges (white arrows) are sharply enhanced, with clear textural contrast between crests (high entropy) and interdune plains (low entropy). **d)** Simple local relief (SLR) model; dune boundaries are also visible, though with a different textural emphasis. **e)** Detail of a sector of the local entropy map (c) to illustrate how the linear pattern closes in a hook, which are interpreted as the arms and noses of parabolic dunes, respectively. **f)** Sketches of the different types of parabolic dunes recognized in the study areas (after Pye, 1993). This result demonstrates the method's efficacy in highlighting subtle organized morphologies.

DISCUSSION

The DemEntropy tool developed here constitutes a novel method that applies a local entropy filter to a DEM to quantify topographic heterogeneity and highlight organized geomorphic patterns. The application of this technique in study cases of the Pampa plain (southern South America) enabled the identification of an extensive field of barely mentioned wind-derived landforms northeast of the Tandilia range (*i.e.*, LMB unit) and improved previous interpretation of aeolian dunes in western Buenos Aires Province (*i.e.*, CPD unit). The interpretation of aeolian dunes is supported by both the surface morphology and the dominant aeolian sediment that blankets the Pampa plain, which exhibits distinctive grain-size and morphostructural characteristics in the two study areas.

Regionally, the CPD unit, western Buenos Aires Province, has a surficial sediment cover dominated by fine-very fine sand and silty sand (Iriondo and Kröhling, 1995). The parent materials of the region's most extensive modern soils were described as loam and silty loam deposits (Camilión and Imbellone, 1984; INTA, 1989; Imbellone and Gimenez, 1998). Particular evidence comes from field sedimentary sections, surveyed by Messineo *et al.* (2019) and Scheifler *et al.* (2024) in two localities of the CPD unit, which expose the nature and age of this aeolian cover (Fig. 5). Two sections, Loma Alta and

Suriano sites, illustrate the dune nose deposits, composed of fine-very fine sand to silty sand, with traces of clay, in massive or weakly laminated beds (Fig. 5). The sedimentary sections at Cabeza de Buey and Laguna Chica sites are located at slightly lower topographic elevations than the previous ones, and are laterally associated with shallow lakes. There, the deposits are dominated by massive, fine-very fine sand, silty sand, and sandy silt, with an average slightly finer texture than at Loma Alta and Suriano sections (Fig. 5). A detailed depositional-postdepositional analysis of both areas, which is out of the scope of this work, is provided in Messineo *et al.* (2019) and Scheifler *et al.* (2024).

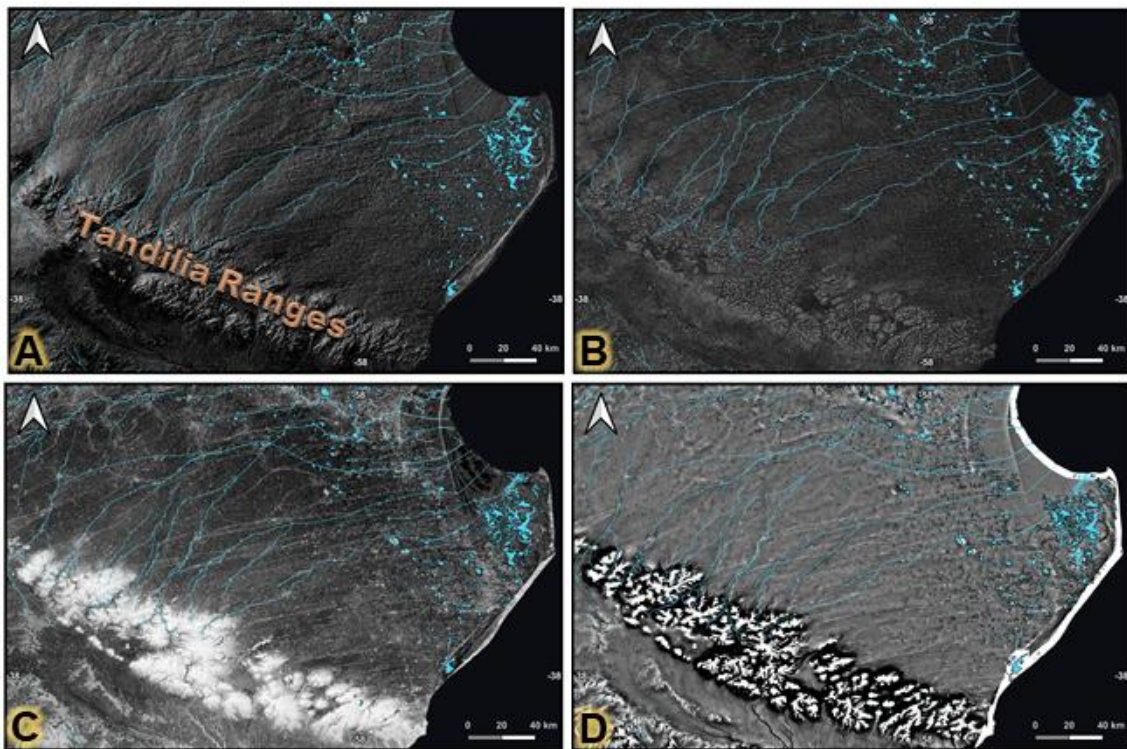


Figure 4. Revelation of aeolian landforms in the LMB unit east of the Tandilia Range (Zone 2 in Fig. 1). **a)** Standard hillshade model (azimuth 315°) shows a seemingly featureless plain. **b)** Sky-view factor (SVF) map reveals no coherent pattern. **c)** Local entropy map (same parameters as Fig. 3c) uncovers an extensive field of well-organized, linear to curvilinear high-entropy ribbons, interpreted as parabolic dunes. Their predominant E-W orientation suggests a westerly paleowind direction. **d)** Simple local relief (SLR) model also highlights these features, independently corroborating the interpretation. The stark contrast between panels (c–d) and (a–b) underscores the power of local entropy analysis and SLR for detecting cryptic aeolian patterns.

The most superficial aeolian deposits along the CPD unit are inferred to be, at least, Late Pleistocene to early Late Holocene in age (Tripaldi and Zárate, 2016; Messineo *et al.*, 2019; Scheifler *et al.*, 2024; Fig. 5) and the dunes on top are mostly stabilized under present climatic conditions. The dune morphologies have been subsequently largely obscured by pedogenesis, erosion (deflation and local runoff), vegetation, and land use (mainly agriculture).

In the CPD aeolian unit there is an agreement between the types, sizes, and orientation of the parabolic dunes exposed in the entropy map with the previously mapped dune morphologies (Contreras *et al.*, 2018; Messineo *et al.*, 2019; Tripaldi *et al.*, 2025), confirming that the entropy signal effectively captures the textural signature of these aeolian features. The entropy map also exposes a coherent dune orientation, reinforcing the interpretation of a sand transport towards the NE.

The entropy map of the northeastern piedmont of the Tandilia range, from the LMB unit, constitutes the most significant outcome of this analysis with the discovery of an extensive and previously unrecognized assemblage of aeolian landforms at a regional scale. Few previous authors mentioned the presence of aeolian landforms in the LMB unit. In the low Pampa, Tricart (1973) documented longitudinal features based on field observations and aerial photography (several-km-long, 1-1.5 m high, and some hundred meters wide), associated with parabolic dunes on the NE margin of blowouts and shallow lakes. Martínez *et al.* (2001) described longitudinal dunes, mega-parabolic dunes, and parabolic dunes in the eastern sector of the Tandilia piedmont, by using RADARSAT-1 and Landsat TM data. Finally, Zárate and Mehl (2010) recognized longitudinal dunes and SE-NE-oriented parabolic dunes, with dune noses closing to the NE, in aerial photographs (see Fig. 5 in Zárate and Tripaldi, 2012), in the distal fluvial basin of the Arroyo del Azul, a stream draining the Tandilia range (Fig. 4). Zárate and Mehl (2010) found the dune ridges are composed of massive sandy silt (described as sandy loess).

According to the DemEntropy map, we infer that the longitudinal aeolian landforms documented in these publications may correspond to the several-km-long arms of the parabolic dunes interpreted here, given the common presence of curvilinear ridges, which stand for the nose dune. This pattern also resembles hairpin parabolic dunes which commonly have km-long arms (Pye and Tsoar, 2009). However, it cannot be ruled out that, besides the presence of parabolic dunes, some of the linear features of the LMB unit correspond to aeolian streaks (McKee, 1979; Cohen-Zada, *et al.*, 2016), which function as aeolian sand transport pathways or to some kind of longitudinal aeolian features. Further studies are needed to test this hypothesis.

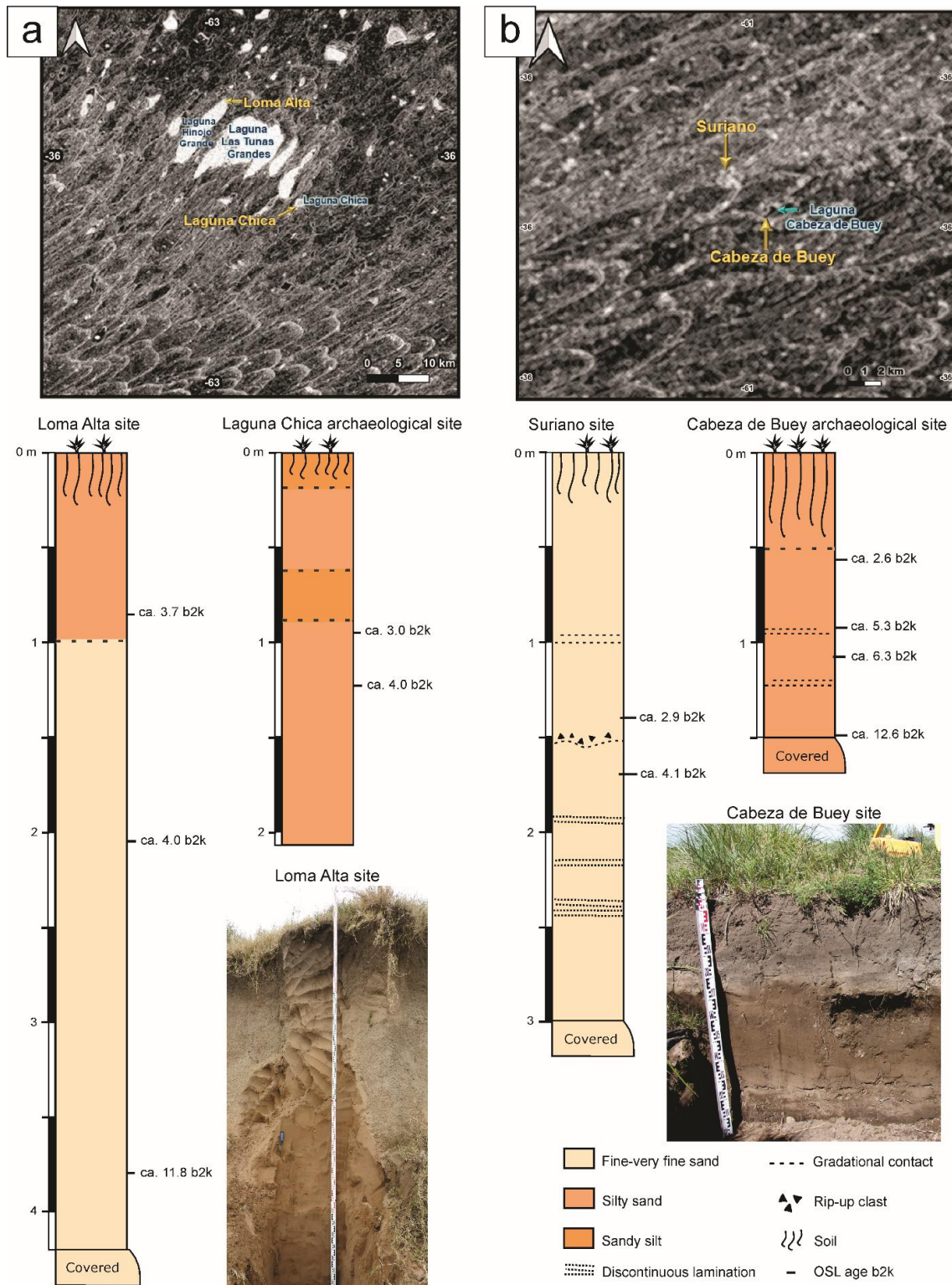


Figure 5. Sedimentological and chronological information from four field-sites located in the study area. **a)** DemEntropy map of a sector of the CPD unit with the location of Loma Alta and Laguna Chica sedimentary sections, which are illustrated below (from Scheifler et al., 2024), accompanied by a picture of the deposit at Loma Alta (photo by A. Tripaldi, May 2019). **b)** DemEntropy map of a sector of the LMB unit with the location of Suriano and Cabeza de Buey

sedimentary sections, which are illustrated below (from Messineo *et al.*, 2019), and a picture of the deposit at Cabeza de Buey (photo by A. Tripaldi, November 2015). Loma Alta and Suriano sections are placed at the nose area of parabolic dunes, and Laguna Chica and Cabeza de Buey are archaeological sites next to shallow lakes developed in the deflation basins of parabolic dunes. The sections expose the nature of the upper 1.5 to 4 m sedimentary cover, composed of fine-very fine sand, silty sand, and sandy silt, with traces of clay (1 to 6%), in massive or discontinuous laminated beds that support the present soils. The chronology is based on luminescence ages, expressed as Years before year 2000 CE (b2k) (Cabeza de Buey and Suriano from Messineo *et al.*, 2019, Loma Alta and Laguna Chica from Scheifler *et al.*, 2024).

Regarding the surficial sediment cover, the Tandilia Range piedmont represents a different grain-size scenario, with loess, sandy loess, and loessial sediments as the dominant cover, particularly in the interfluvial plains between the small arroyos that drain the piedmont (Iriondo and Kröhling, 1995; Zárate, 2003). This sediment cover is texturally unsuitable for the development of aeolian dunes (Livingstone and Warren, 2019). Dust deposition, in the form of mantles, mainly occurs through wash out by rainfall, while dry dust deposition is related to topographic obstacles or an increase of surface roughness due to vegetation (Pye and Tsoar, 1987). Bedforms associated with this type of aeolian sedimentation are neither expected nor have they been described as loess aggradation blankets on pre-existing relief. Thus, the recognized aeolian features pose a challenge for interpretation. A possible answer is that the Holocene aeolian morphogenesis recognized in the western and central Pampa (*e.g.*, Forman *et al.*, 2014; Messineo *et al.*, 2019; Scheifler *et al.*, 2024) also affected this area. It is hypothesized that southwesterly winds partially reworked the loess and sandy loess mantles or, more likely, set into saltation fine-very fine sand and coarse silty sand from the alluvial plain of the arroyos that drain the Tandilia piedmont. The limited sand available would have triggered the formation of the observed type of parabolic dunes with skinny, extremely long arms. Further research, including an extensive field survey and granulometric laboratory determination, is needed to test this hypothesis based on the use of the novel remote sensing tool presented here.

The recognized parabolic dune pattern can be morphologically compared with parabolic dunes from the White Sand Dunes (New Mexico, USA), a well-known and widely studied example of parabolic dunes (Baitis *et al.*, 2014 and references therein). The southern area of this dunefield is dominated by parabolic dunes with patterns that show noticeable similarities with those of the parabolic dunes from the Pampa plain (Fig. 6). In the White Sand Dunes, near the provenance area from where the dunes blow up to the NE, there are few elongated parabolic dunes, with longer arms and a lower density of dunes per square kilometer (Fig. 6c) when compared to the dune pattern of the more distal eastern sector (Fig. 6a). The first dune pattern is similar to the one along the northern piedmont of the Tandilia range (Fig. 6d). In comparison, the tighter dune pattern looks like the parabolic dunefield of the CPD units (Fig. 6b).

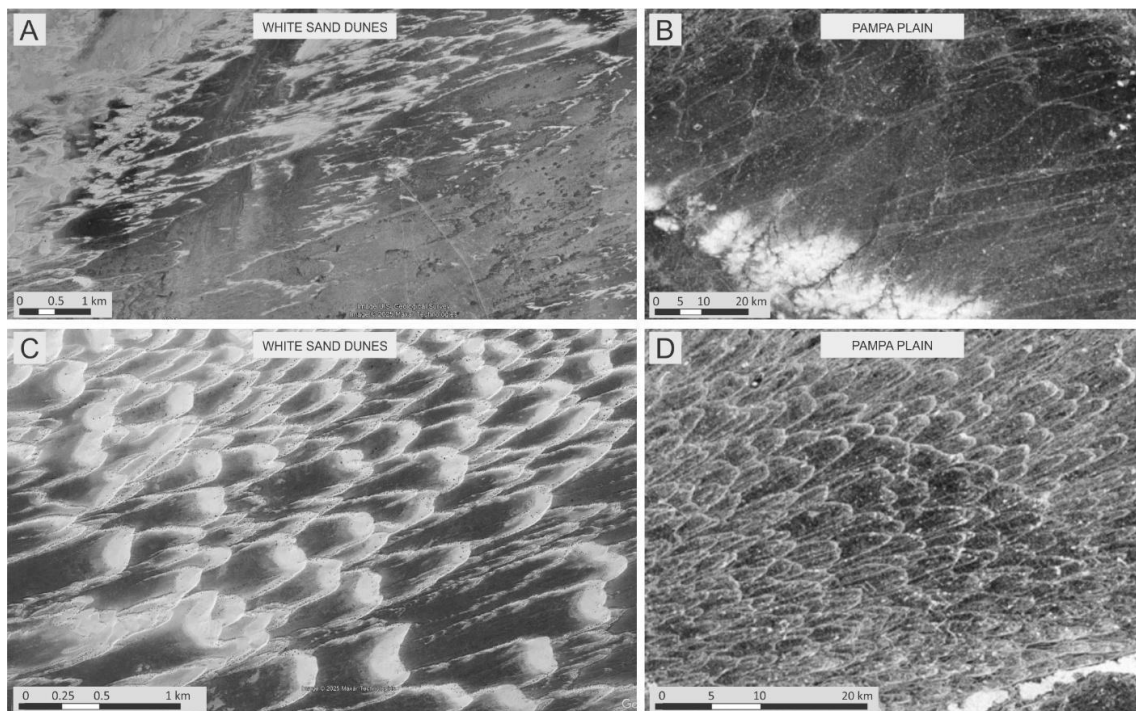


Figure 6. Comparison of dune patterns between White Sands (New Mexico, USA) and the Pampa plain. The southern area of White Sands is dominated by parabolic dunes with patterns that show noticeable similarities to those analyzed in the Pampa plain. In proximal source areas, elongated parabolic dunes with longer arms and lower density predominate (**a**) White Sands; **b**) Pampa plain), whereas the more distal eastern sector exhibits a tighter dune pattern (**c**) White Sands; **d**) Pampa plain). Satellite images of White Sands from Baitis *et al.* (2014).

It is inferred that the two dune patterns primarily reflect the differing grain sizes of the sediment that blanket both aeolian units –sandier in CPD and siltier in LMB– as well as the distinct aeolian morphogenesis, likely triggered by different morphostructural contexts and Quaternary evolution in both areas. Similar to the White Sand Dunes, the CPD is in the distal position of the sand provenance area, that is, the Desaguadero alluvial plain in western La Pampa Province (Iriondo, 1990), from where the sand was transported along the aeolian corridors of the Valles Transversales of La Pampa Province (Tripaldi *et al.*, 2018). Meanwhile, the parabolic dunes in the LMB unit are locally developed, due to the reworking of previous aeolian units and of fluvial sediments of the Tandilia piedmont (Zárate and Mehl, 2010).

In terms of remote sensing analysis, the powerful contrast between the featureless hillshade and sky-view factor and the richly detailed entropy map underscores the efficacy of local entropy analysis for geomorphological mapping. The method's success lies in its fundamental property: it ignores absolute elevation and instead quantifies the spatial complexity or texture of the topographic signal. Aeolian bedforms, even when topographically subdued, retain a highly organized, repetitive texture that generates a predictable entropy signature. This makes the proposed technique suited for detecting low-amplitude, large-wavelength features that are invisible to methods reliant on slope or gradient, which are often minimal in such landscapes. The DemEntropy package effectively operationalizes this theoretical principle into a practical and accessible tool.

While powerful, the method is not without limitations. The choice of parameters (r , δ) influences the scale and type of features detected, requiring an understanding of the target geomorphology. The technique may also highlight other patterned terrains, such as those produced by forests, infrastructure, and large-scale cultivation, necessitating a careful interpretation.

The comparison with other terrain visualization techniques reveals that DemEntropy and simple local relief (SLR) produce strikingly similar patterns

in both study areas, independently validating the geomorphological interpretation. While SLR is a well-established method that highlights local elevation variability, DemEntropy offers a complementary perspective by quantifying the spatial organization of the topographic signal based on information theory. Moreover, DemEntropy incorporates a shift-averaging procedure that mitigates discretization artifacts and provides a clear theoretical link to the concept of textural complexity. In contrast, sky-view factor (SVF) yielded limited enhancement for the low-relief features investigated here, reinforcing the suitability of texture-based approaches for mapping subtle aeolian landforms.

Future work should focus on exploring the application of the tool to other cryptic landscapes, such as glacial or fluvial terrains, and on hybrid approaches that combine the computational efficiency of DemEntropy with more advanced pattern recognition techniques, such as the deep learning and skeletonization workflow recently developed by Daynac *et al.* (2024), to achieve fully automated dune feature extraction.

CONCLUSIONS

This study has successfully demonstrated that local entropy analysis, operationalized through the novel DemEntropy software package, provides a powerful approach for mapping subtle aeolian landforms in low-relief, vegetated landscapes. The technique's fundamental innovation lies in its shift from analyzing absolute elevation to quantifying topographic texture, allowing it to reveal organized geomorphic patterns that are otherwise invisible to conventional DEM visualization techniques.

The application of this method to the TanDEM-X DEM of the Pampa plain yielded two principal outcomes of high scientific value. First, it served as a robust evaluation, dramatically enhancing the visibility and delineation of known parabolic dunefields within the Pampean Sand Sea and confirming the method's efficacy. Second, and most significantly, it led to a discovery: the

identification of an extensive, previously undocumented assemblage of aeolian features northeast of the Tandilia range, also with a parabolic dune pattern. This finding alone calls for a revision of the existing geomorphological paradigm for the region, pointing to a more extensive and complex history of Quaternary aeolian activity than previously recognized.

Beyond the specific findings in the Pampas, the broader contribution of this work is the provision of DemEntropy as a free, open-source, and community-ready tool. By packaging the algorithm into an easy-to-install Python package, we ensure the reproducibility of our results and guarantee its accessibility to researchers across the geosciences, regardless of their computational expertise. The method's simplicity and power suggest it has considerable potential for application to a wide range of other cryptic landscapes, from glacial and fluvial terrains on Earth to planetary surfaces.

In conclusion, this research underscores the profound insights that can be gained by applying novel computational and theoretical frameworks to existing geospatial data. The DemEntropy tool provides a new lens through which to view the landscape, one that reveals the faint but structured textural imprint of past processes, ultimately enabling a more complete interpretation of Earth's surface history.

Acknowledgments. The authors are grateful to P. Minotti for suggesting the interaction that led to this collaboration. This research was supported by grants PICT-ANPCyT 2020-A-04001 (to R.G), PIP-CONICET 11220210100052CO (to A.T.) and 11220200100887CO (to R.G). The authors thank the two reviewers and the editor for their comments and suggestions, which helped to improve the quality of our manuscript.

REFERENCES

- Almutlaq, F., and Mulligan, K. (2023). Using texture statistics to identify and map different dune types within the Rub'al Khali. *Remote Sensing*, 15(19), 4653. <https://doi.org/10.3390/rs15194653>

- Baitis, E., Kocurek, G., Smith, V., Moring, D., Ewing, R. C., and Peyret, A. P. B. (2014). Definition and origin of the dune-field pattern at White Sands, New Mexico. *Aeolian Research*, 15, 269–287. <https://doi.org/10.1016/j.aeolia.2014.06.004>
- Benzaquén, L., Lingua, G., Firpo Lacoste, F., and Gonzalez Trilla, G. (2020). *Documento marco para el desarrollo del Inventario Nacional de Humedales de Argentina*. Ministerio de Ambiente y Desarrollo Sostenible de Argentina, 56 pp, Buenos Aires.
- Camilión, M. C., and Imbellone, P. A. (1984). Caracterización de los materiales constituyentes de algunos suelos del partido de Carlos Tejedor Provincia de Buenos Aires. *Ciencia del Suelo* 2, 137–148.
- Contreras, F. I., Manstretta, M. G. M., Perillo, G. M. E., and Piccolo, M. C. (2018). Caracterización de médanos parabólicos de la región pampeana oriental, centro oeste de la provincia de Buenos Aires (Argentina). *Latin American Journal of Sedimentology and Basin Analysis*, 25(1), 1–15.
- Cohen-Zada, A. L., Blumberg, D. G., Maman, S., 2016. Earth and planetary aeolian streaks: A review. *Aeolian Research* 20, 108–125. <https://doi.org/10.1016/j.aeolia.2015.12.002>
- Courech du Pont, S., Rubin, D. M., Narteau, C., Lapôtre, M. G., Day, M., Claudin, P., Livingstone, I., Telfer, M. W., Radebaugh, J., Gadal, C., Gunn, A., Hesp, P. A., Carpy, S., Bristow, C. S., Baas, A. C. W., Ewing, R. C., and Wiggs, G. F. S. (2024). Complementary classifications of aeolian dunes based on morphology, dynamics, and fluid mechanics. *Earth-Science Reviews*, 104772. <https://doi.org/10.1016/j.earscirev.2024.104772>
- Daynac, J., Bessin, P., Pochat, S., Mourgues, R., and Shumack, S. (2024). A new workflow for mapping dune features (outline, crestline and defects) combining deep learning and skeletonization from DEM-derived data. *Geomorphology*, 463, 109369. <https://doi.org/10.1016/j.geomorph.2024.109369>
- Dangavs, N. V. (1979). Presencia de dunas de arcilla fósiles en la Pampa Deprimida. *Revista de la Asociación Geológica Argentina*, 34(1), 31–35.
- Forman, S. L., Tripaldi, A., and Ciccioli, P. L. (2014). Eolian sand sheet deposition in the San Luis paleodune field, western Argentina as an indicator of a semi-arid environment through the Holocene. *Palaeogeography, Palaeoclimatology, Palaeoecology*, 411, 122–135. <https://doi.org/10.1016/j.palaeo.2014.05.038>
- Frenguelli, J. (1955). *Loess y limos pampeanos* (Serie Técnica y Didáctica N° 7, 88 pp.). Ministerio de Educación de la Nación.
- Hesse, R. (2010). LiDAR-derived Local Relief Models – a new tool for archaeological prospection. *Archaeological Prospection*, 17, 67–72. <https://doi.org/10.1002/arp.374>
- INTA (1989). *Mapa de suelos de la provincia de Buenos Aires. Escala 1:500.000*. Centro de Investigación de Recursos Naturales (CIRN), Instituto Nacional de Tecnología Agropecuaria e Instituto de Evaluación de Tierras, Castelar.
- Imbellone, P. A., and Giménez, J. E. (1998). Parent materials, buried soils and fragipans in northwestern Buenos Aires Province, Argentina. *Quaternary International* 51-52, 115–126. [https://doi.org/10.1016/S1040-6182\(97\)00038-4](https://doi.org/10.1016/S1040-6182(97)00038-4)

- Iriondo, M. H. (1990). Map of the South American plains—its present state. In J. Rabassa (Ed.), *Quaternary of South America and Antarctic Peninsula* (pp. 297–308). Balkema. <https://doi.org/10.1201/9781003079484>
- Iriondo, M. H., and Kröhling, D. M. (1995). El sistema eólico pampeano. *Comunicaciones del Museo Provincial de Ciencias Naturales “Florentino Ameghino”*, 5(1), 1–68.
- Kokalj, Ž., and Somrak, M. 2019. Why Not a Single Image? Combining Visualizations to Facilitate Fieldwork and On-Screen Mapping. *Remote Sensing* 11(7), 747. <https://doi.org/10.3390/rs11070747>
- Livingstone, I., and Warren, A., 2019. *Aeolian geomorphology: A New Introduction*. Wiley & Sons, 318pp. 10.1002/9781118945650
- Malagnino, E. C. (1989). *Paleoformas de origen eólico y sus relaciones con los modelos de inundación de la provincia de Buenos Aires [Abstract]*. IV Simposio Latinoamericano de Percepción Remota y IX Reunión Plenaria SELPER, Tomo II (pp. 611–620). San Carlos de Bariloche, Argentina.
- Martínez, G. A., Arca, J. M., Gwyn, Q. H. J., and Bernasconi, M. V. (2001). Combined use of RADARSAT-1 and Landsat TM data for geomorphological applications in lowlands of Buenos Aires Province, Argentina. *Canadian Journal of Remote Sensing*, 27(6), 638–642. <https://doi.org/10.1080/07038992.2001.10854905>
- McKee, E. D. (1979). *A study of global sand seas* (Professional Paper 1052, 429 pp.). U.S. Geological Survey. <https://doi.org/10.3133/pp1052>
- Melton, F. A. (1940). A tentative classification of sand dunes its application to dune history in the Southern High Plains. *The Journal of Geology*, 48(2), 113–174. <https://doi.org/10.1086/624871>
- Messineo, P. G., Tonello, M., Stutz, S., Tripaldi, A., Scheifler, N., Pal, N., Sánchez Vuichard, G., and Navarro, D. (2019). Human occupations and related environment-climate during the Middle and Late Holocene in central Pampas of Argentina. *The Holocene*, 29(2), 244–261. <https://doi.org/10.1177/0959683618810407>
- Morley, A. M., Mather, T. A., Pyle, D. M., and Kendall, J. M. (2025). Detecting shallow subsurface anomalies with airborne and spaceborne remote sensing: A review. *Science of Remote Sensing*, 11, 100187. <https://doi.org/10.1016/j.srs.2024.100187>
- Oyarzabal, M., Clavijo, J., Oakley, L., Biganzoli, F., Tognetti, P., Barberis, I., Maturo, H. M., Aragón, R., Campanello, P. I., Prado, D., Oesterheld, M. and León, R. J. C. (2018). Unidades de vegetación de la Argentina. *Ecología Austral*, 28(1), 40–63. <https://doi.org/10.25260/EA.18.28.1.0.399>
- Piovano, E. L., Stutz, S., Morales, J. A., and Ariztegui, D. (2025). Introducing Pampean Lakes. In F. R. Miranda, A. M. del Puerto, and H. E. Massone (Eds.), *Pampean Lakes* (pp. 1–12). Springer. https://doi.org/10.1007/978-3-031-86028-7_1
- Pye, K. (1993). Late Quaternary development of coastal parabolic megadune complexes in northeastern Australia. In K. Pye and N. Lancaster (Eds.), *Aeolian sediments* (pp. 23–44). Blackwell Publishing Ltd. <https://doi.org/10.1002/9781444303971.ch3>

- Pye, K., and Tsoar, H. (1987). The mechanics and geological implications of dust transport and deposition in deserts with particular reference to loess formation and dune sand diagenesis in the northern Negev, Israel. *Geological Society of London*, 35(1), 139–156. <https://doi.org/10.1144/GSL.SP.1987.035.01.10>
- Pye, K., and Tsoar, H. (2009). *Aeolian Sand and Sand Dunes*. Springer, 475 pp.
- Scheifler, N., Ozán, I. L., Tripaldi, A., González, M. E., Valero, F. S., Marini, N., Politis, G. G., and Messineo, P. G. (2024). Formation processes and environments in the Hinojo-Las Tunas shallow lake system, Argentina Pampas: The Laguna Chica archaeological locality as a case study. *Geoarchaeology*, 40(6), e22034. <https://doi.org/10.1002/gea.22034>
- Shannon, C. E. (1948). A mathematical theory of communication. *The Bell System Technical Journal*, 27(3), 379–423. <https://doi.org/10.1002/j.1538-7305.1948.tb01338.x>
- Tricart, J. L. (1973). *Geomorfología de la Pampa Deprimida*. Base para los estudios edafológicos y agronómicos. Instituto Nacional de Tecnología Agropecuaria (INTA), Vol. XII Colección Científica 12. Buenos Aires, pp. 202
- Tripaldi, A., and Zárate, M. A. (2016). A review of Late Quaternary inland dune systems of South America east of the Andes. *Quaternary International*, 410, 96–110. <https://doi.org/10.1016/j.quaint.2014.06.069>
- Tripaldi, A., Forman, S. L., and Badger, T. (2018). Parabolic megadunes in a subtropical Quaternary inland dune field, southwestern Pampas, Argentina. *Geomorphology*, 303, 396–406. <https://doi.org/10.1016/j.geomorph.2018.08.021>
- Tripaldi, A., Zárate, M. A., and Gallo, M. (2025). Aeolian origin of the Pampean lakes of central Argentina, southern South America: A Quaternary wind legacy to a wet-dry changing landscape. In E. L. Piovano, S. Stutz, J. A. Morales, and D. Ariztegui (Eds.), *Pampean Lakes* (pp. 123–150). Springer. https://doi.org/10.1007/978-3-031-86028-7_6
- Van der Walt, S., Schönberger, J. L., Nunez-Iglesias, J., Boulogne, F., Warner, J. D., Yager, N., Gouillart, E., Yu, T., and the scikit-image contributors (2014). Scikit-image: Image processing in Python. *PeerJ*, 2, e453. <https://doi.org/10.7717/peerj.453>
- Viglizzo, E. F., and Frank, F. C. (2006). Ecological interactions, feedbacks, thresholds and collapses in the Argentine Pampas in response to climate and farming during the last century. *Quaternary International*, 158(1), 122–126. <https://doi.org/10.1016/j.quaint.2006.05.022>
- Wessel, B. (2018). *TanDEM-X ground segment–DEM products specification document*. Public Document TD-GS-PS-0021, Issue 3.2. EOC, DLR, Oberpfaffenhofen, Germany. <https://elib.dlr.de/223711/>
- Zárate, M. A. (2003). Loess of southern South America. *Quaternary Science Reviews*, 22(17–18), 1987–2006. [https://doi.org/10.1016/S0277-3791\(03\)00165-3](https://doi.org/10.1016/S0277-3791(03)00165-3)
- Zárate, M. A. (2005). El Cenozoico tardío continental de la provincia de Buenos Aires. In R. E. de Barrio, R. O. Etcheverry, M. F. Caballé and E. Llambías (Eds.), *Geología y recursos minerales de la provincia de Buenos Aires*. Relatorio del 16° Congreso Geológico Argentino (pp. 139–158). La Plata.

- Zárate, M. A. (2009). El paisaje pampeano a través del tiempo. In M. A. Berón, M. Bonomo, and L. H. Luna (Eds.), *Mamul Mapu: Pasado y presente desde la arqueología pampeana* (pp. 215–228). Libros del Espinillo, Ayacucho, Buenos Aires. 978-987-25159-4-2
- Zárate, M. A., and Mehl, A. (2010). *Geología y geomorfología de la cuenca del arroyo del Azul, provincia de Buenos Aires, Argentina*. I Congreso Internacional de Hidrología de Llanuras: Actas (pp. 81–94). Azul, Buenos Aires, Argentina.
- Zárate, M. A., and Tripaldi, A. (2012). The aeolian system of central Argentina. *Aeolian Research*, 3(4), 401–417. <https://doi.org/10.1016/j.aeolia.2011.08.002>
- Zakšek, K., Oštir, K., and Kokalj, Ž. (2011). Sky-View Factor as a Relief Visualization Technique. *Remote Sensing*, 3(2), 398-415. <https://doi.org/10.3390/rs3020398>
- Zheng, Z., Du, S., Taubenböck, H., and Zhang, X. (2022). Remote sensing techniques in the investigation of aeolian sand dunes: A review of recent advances. *Remote Sensing of Environment*, 271, 112913. <https://doi.org/10.1016/j.rse.2022.112913>